$\pi^- - p$ Interactions at 683 MeV/c†

R. A. BURNSTEIN, G. R. CHARLTON, T. B. DAY, G. QUARENI,*
A. QUARENI-VIGNUDELLI,* AND G. B. YODH‡
Department of Physics and Astronomy, University of Maryland, College Park, Maryland

AND

I. NADELHAFT
Carnegie Institute of Technology, Pittsburgh, Pennsylvania

(Received 5 October 1964)

Interactions of 683-MeV/c negative pions with protons were investigated using the BNL 14-in. hydrogen bubble chamber in a 17-kG field. Two thousand elastic scatterings were analyzed, yielding a cross section of 18.9±1.0 mb. No evidence for powers of cos θ higher than the second was observed in the elastic angular distribution. The angular distribution obtained was $d\sigma/d\omega = (0.384\pm0.026)+(1.70\pm0.06)\cos\theta+(3.36\pm0.11)\cos^2\theta$ mb/sr. The single-pion production reactions $\pi^-+p\rightarrow\pi^-+\pi^0+p$ and $\pi^-+p\rightarrow\pi^-+\pi^+ +n$ were studied in detail. A total of 441 π^0 productions and 833 π^+ productions were analyzed giving cross sections of 3.99±0.50 and 7.50±0.80 mb, respectively. The differential distributions for these inelastic processes are presented and compared with the predictions of the model of Olsson and Yodh. The distribution of events on the Dalitz plots for π^0 production is accounted for by the model. However, for the π^+ reaction, the model (so far developed) does not describe adequately the distribution of events on the Dalitz plot. In particular, the model fails to account for the enhancement at high $(\pi^+\pi^-)$ effective masses in $\pi\pi$ mass distribution. The center-of-mass angular distributions for π^0 and π^+ production reactions are presented and compared with the model.

I. INTRODUCTION

A STUDY of $\pi^- - p$ interaction at 683 MeV/c is reported in this paper.[1] It was undertaken as a part of a comprehensive survey of π^+ and π^- interactions in hydrogen from 450 MeV to 1 BeV pion kinetic energy,[2] using the 14-in. Brookhaven National Laboratory bubble chamber. Bubble-chamber technique is well suited to the study of elastic and charged inelastic channels, and it was the purpose of this survey to provide information on the charged inelastic channels of accuracy comparable to that of previous experiments for the elastic,[3] charge exchange,[4] inelastic neutral[5,6] channels. It was hoped that all the data obtained would lead to a real understanding of the nature of the higher maxima (at 600 and 900 MeV) in the $\pi^- p$ system.

The reactions that have been studied in this experiment are

$$\pi^-+p\rightarrow\pi^-+p \quad \text{elastic scattering} \quad (1)$$

$$\pi^-+p\rightarrow\pi^-+\pi^0+p \quad \text{single } \pi^0 \text{ production} \quad (2)$$

$$\pi^-+p\rightarrow\pi^-+\pi^++n \quad \text{single } \pi^+ \text{ production} \quad (3)$$

$$\pi^-+p\rightarrow \text{neutrals} \quad \text{charge exchange plus } \pi^0 \text{ production} \quad (4)$$

$$\pi^-+p\rightarrow \text{multipion production.} \quad (5)$$

The total cross sections for reactions (1) through (4) and an upper limit to the multipion cross section have been measured. The elastic angular distribution has been obtained and compared with previous measurements. The inelastic reactions (2) and (3) have been studied in detail and relevant three-body differential distributions are presented.

In Sec. V the data for reactions (2) and (3) are compared with the phenomenological analysis of single pion production in pion nucleon collisions of Olsson and Yodh.[7]

II. EXPERIMENTAL

A. Beam

A negative pion beam at 32° from the "jump" target in the south straight section of the Cosmotron at Brookhaven National Laboratory was used. The beam

† Supported in part by the U. S. Atomic Energy Commission.
* Present address: Institute of Physics, Bologna, Italy.
‡ Also at Brookhaven National Laboratory, Upton, New York.
[1] Preliminary report was given by R. A. Burnstein, G. R. Charlton, T. B. Day, G. Quareni, A. Quareni-Vignudelli, and G. B. Yodh, University of Maryland Technical Report No. 346, 1964 (unpublished).
[2] These experiments were motivated by a joint effort of Dr. R. K. Adair, L. Leipuiner, H. J. Martin, V. P. Kenney, J. Ashkin, B. Musgrave, R. Chrittenden, and G. B. Yodh.
[3] J. A. Helland, T. J. Devlin, D. E. Hagge, M. J. Longo, B. J. Moyer, and C. D. Wood, in *Proceedings of the 1962 Annual International Conference on High Energy Physics at CERN*, edited by J. Prentki (CERN, Geneva, 1962), p. 3, and Phys. Rev. **134**, B1079 (1964). References to earlier work are contained in this paper.
[4] J. F. Detoeuf, Y. Ducros, J. P. Merlo, A. Sterling, B. Thevenet, L. Van Rossum, and J. Zsembevy, in *Proceedings of the 1962 Annual International Conference on High Energy Physics at CERN*, edited by J. Prentki (CERN, Geneva, 1962), p. 7 and Phys. Rev. **134**, B228 (1964); B. C. Barish, R. J. Kurz, Victor Perez-Mendez, and Julius Solomon, *ibid.* **135**, 13416 (1964).
[5] R. Turlay Rapport CEA No.: 2136, Saclay (unpublished) and R. Kurz, University of California Radiation Laboratory Report No. UCRL-10564 (unpublished).
[6] P. Falk-Vairant and G. Valladas, Rev. Mod. Phys. **33**, (1961) 362; C. D. Wood, T. J. Devlin, J. A. Helland, M. J. Longo, B. J. Moyer, and V. Perez-Mendez, Phys. Rev. Letters **6**, 481 (1961).
[7] M. Olsson and G. B. Yodh, Phys. Rev. Letters **10**, 353 (1963); Bull. Am. Phys. Soc. **9**, 27 (1964); University of Maryland Technical Report No. 358, 1964 (unpublished); and M. Olsson, University of Maryland Technical Report No. 379, 1964 (unpublished).

set up is shown in Fig. 1. The beam was designed to give a pion beam from 0.4 to 1 BeV/c momentum and about $\pm 1\%$ momentum spread.[8] There was a double focus at the bubble chamber, with a horizontal magnification of 0.89 and a vertical magnification of 2.47. The total length of the beam was 765 in. By rf notching[9] the beam was operated parasitically using about 5% of the internal proton beam.

The beam contamination from 500 to 800 MeV/c was determined using a 3-in.-long CO_2 threshold Čerenkov counter placed 10 ft upstream from the bubble-chamber position. The percentage of muon and electron contamination as a function of momentum is shown in Fig. 2.

B. Bubble Chamber

The pion beam traversed the 14-in.-diam, 8-in.-deep BNL hydrogen bubble chamber with a magnetic field

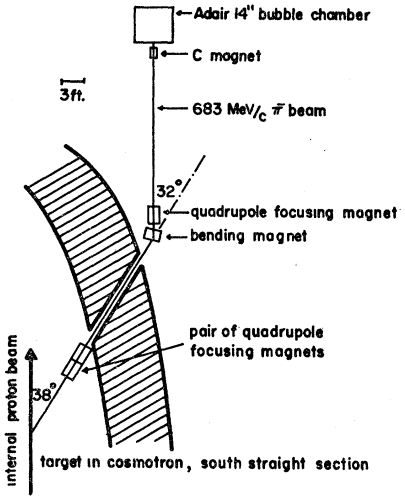

FIG. 1. The beam layout.

at the center of the chamber of 17.45 kG. The beam was spatially contained in a region ± 2 in. in depth about the median plane of the chamber. A total of 25 000 pictures were taken with about 20 tracks per frame.

C. Fiducial Region and Beam Track Criteria

In order to insure good identification and measurement of tracks, the fiducial region shown in Fig. 3 and defined in view 1 was used. The lines AA and BB were normal to the chord subtended by a typical beam track crossing these lines. Approximately 80% of all good (defined below) beam tracks were in this region. The average path length of each track was equal to 19.276 cm.

[8] For details of the beam, see C. N. Vittitoe, thesis, University of Kentucky, 1963 (unpublished); C. N. Vittitoe, W. Fickinger, V. P. Kenney, J. Mowat, and W. Shephard, Bull. Am. Phys. Soc. 9, 80 (1964) and Phys. Rev. 135, B232 (1964).

[9] The rf notching technique was developed by L. Leipuiner for this beam.

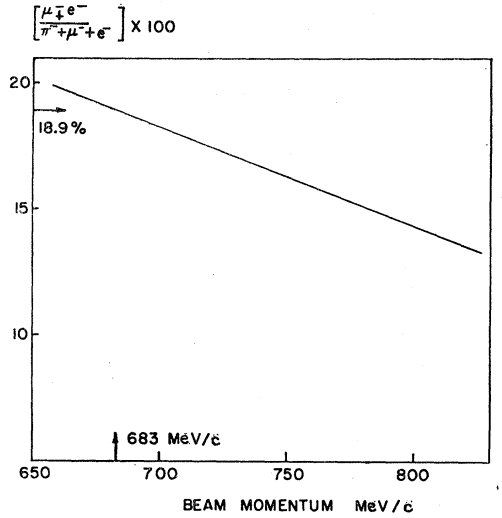

FIG. 2. Muon plus electron contamination of the beam as a function of beam momentum, as determined using a CO_2 Čerenkov counter.

In Fig. 4 is shown a plot of dip versus azimuth (positive dip being away from the cameras and azimuth being measured positive downwards from line joining F_1F_2 on the top glass) for incoming tracks. All tracks having an azimuth within $\pm 2°$ of the average azimuth of 6.4° were used as good beam tracks. This cutoff was carried out on the scanning table for part of the analysis. The cutoff for dip was carried out in the analysis stage and is described in the data-processing section.

D. Beam Momentum

The beam momentum was determined by calculating the incoming pion energy from elastic events where the recoil proton stopped in the chamber. The incoming momentum is calculated from the range of the proton and the scattering angles of the proton and the outgoing pion. The hydrogen density was found from the range of μ^+ from π^+ decay. The weighted average beam mo-

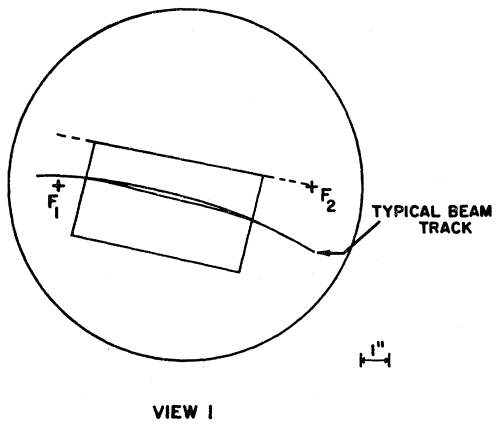

FIG. 3. Fiducial region for the experiment. The region was defined in view 1.

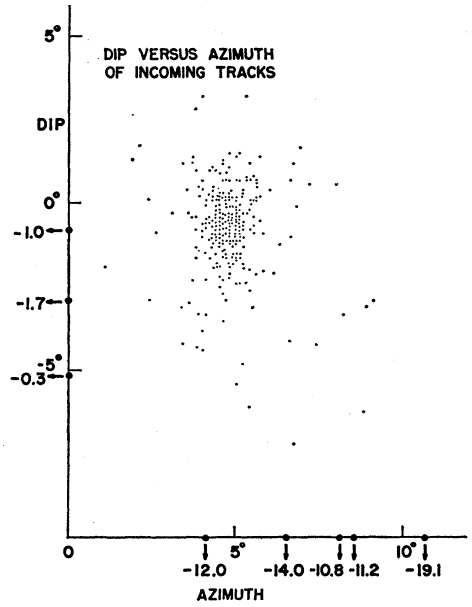

FIG. 4. Angular collimation of beam tracks. The points on the axes correspond to events which were located outside the region covered by the figure. The arrows indicate the direction in which the points lie.

mentum was found to be 683 MeV/c. This was 1% less than the average beam momentum determined from curvature of beam tracks and knowledge of the magnetic field. Therefore, we corrected the magnetic field value by multiplying by 0.99. The beam spread was ± 10 MeV/c. The distribution is shown in Fig. 5.

E. Scanning

The photographs were scanned using three distinct procedures: (a) a $2p$ event scan, (b) a track count, and (c) a $0p$ event scan.

(a) *$2p$ event scan*: Reactions (1)–(3), elastic, single π^0 production, and single π^+ production lead to a two-prong ($2p$) topology. For these events all the film was double scanned and a third was triple scanned. The outgoing positive track was identified to be a proton or a π^+ using ionization and range information. The obvious inelastic events were labeled π^0 or π^+ production depending on the identification of the outgoing positive. The π^0 productions and elastic events were separated, as far as possible, on the scanning table by using crude angle correlations. Frames which had more than 25 tracks or were too faint or blanks were rejected. Only events consistent with the beam track criteria were accepted.

(b) *Track count for $2p$ events*: Every sixth frame was track counted to determine the incident flux. A template with a typical beam track (in view 1) was mounted on a drafting arm, and the scanner was instructed to count only those tracks which had an azimuth angle $\pm 2°$ of the average direction. All tracks regardless of interaction were counted. This count was done only in acceptable frames defined in (a). Thus, it was possible to calculate the absolute cross section roll by roll and check for any scanning biases. All rolls were track counted twice using different frames.

(c) *$0p$ scan*: In order to achieve high efficiency for recording track disappearances in the chamber, only frames with less than 15 good beam tracks were used in the $0p$ scan. In this scan every sixth frame was used for track count. About a third of the total pictures were used in this scan and all were double scanned. We obtained a total neutral cross section from this scan to compare with accurate counter measurements at Saclay.[4]

F. Measuring

The measurements of the events were of two types. About 60% of the events were measured on a digitized microscope stage with five points to a track and the rest were measured by hand reconstruction on scanning table using corresponding points and curvature templates.[10] The accuracy of the hand measurements was better than 0.1 mm on scanning table (magnification of about 15) which was adequate for analysis at these momenta. The χ-square and stretch distributions obtained from the two kinds of measurements are completely consistent.

G. Data Processing

All $2p$ events were measured and kinematical quantities were calculated using reconstruction programs appropriate for each kind of measurement. Only events which satisfied the following geometrical criteria were selected as our sample:

(a) Azimuth of the incoming track was within $\pm 2°$ of the average.

(b) The dip δ was such that

$$\delta \leq 3+175/L^2, \quad \delta>0,$$
$$\delta \geq -(1.75+175/L^2), \quad \delta<0,$$

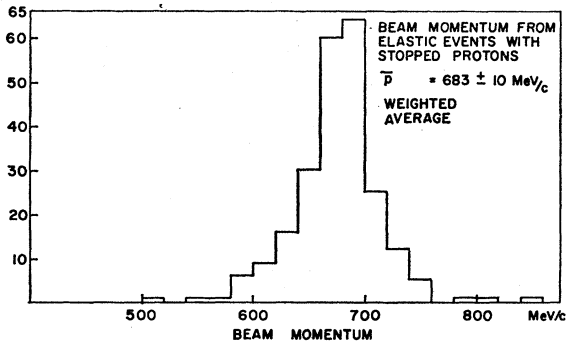

FIG. 5. Distribution of beam momentum as determined from elastic events with recoil protons that stop in the chamber.

[10] V. Borelli, P. Franzini, T. Manelli, A. Minguzzi-Ranzi, R. Santangelo, F. Saporetti, V. Silvestrini, P. Waloschek, and V. Zoboli, Nuovo Cimento **10**, 525 (1958).

where L is the length of the incident pion track in centimeters.

Those events which had been mechanically measured were spatially reconstructed with the DATPRO program of Leipuiner and Adair. A special program was written to reconstruct the hand-measured events, comparable to DATPRO in its output, except that multiple-scattering, straggling, and measurement errors were incorporated. At this stage, the scanning decision of event-type (elastic scattering, π^0 or π^+ production) was used in the assignment of errors to the positive outgoing track and the reconstructed track information was then mass dependent.

The kinematic fitting and hypothesis testing were done by a version of GUTS supplied by Musgrave. All three possibilities of interpretation were tested, and results of the fitting put out for each. Two separate programs did the initial bookkeeping on this output of three fits per event. The first separated the events into three categories: (a) rejects, i.e., no good fit at all; (b) good (confidence level greater than 1%); and (c) ambiguous. All rejects and ambiguous events were remeasured at least once. The good events were rechecked on the scanning table to see if the fitted hypothesis agreed with the scanning decision as to event type. If so, it was accepted; if not, the errors were changed accordingly and the measurements with both sets of errors put through the system again. In the case of ambiguous events, provision was made either to accept the best fit if ionization information was inconclusive or to choose that fit which agreed with the ionization information. After a second remeasurement for some events, a negligible (less than 4%) number of events remained in the reject or ambiguous categories.

The resulting fitted data were checked for biases and for correct error assignments. The most sensitive test of both is to plot the "stretch" quantities[11] where, for some quantity x, the "stretch" function is

$$s(x)=\frac{x_{\text{fit}}-x_{\text{meas}}}{(\sigma_x)_{\text{rms}}}.$$

In Fig. 6 we give as an example perhaps the most useful of these plots for our experiment, the one for the stretch in

$$k=[\text{momentum}\times\cos(\text{dip})]^{-1}$$

for the scattered proton in elastic scattering events where the proton stops. (The smooth curve is a Gaussian, centered at zero and of width one.) The symmetry about zero, and the full width of about one show the correctness of the error assignments and the lack of biases. A further check was made by plotting χ^2 for the different event types. Figure 7 shows such a plot for the 4-constraint case of elastic scattering. The smooth curve is the expected result.

[11] R. Ross, University of California Radiation Laboratory Report No. UCRL-9749, 1961 (unpublished) and W. E. Humphrey, University of California Radiation Laboratory Report No. UCRL-9752, 1961 (unpublished).

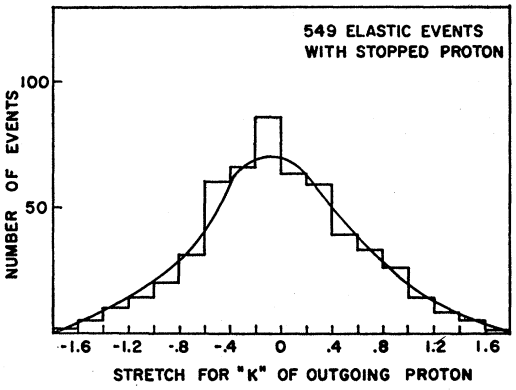

FIG. 6. Distribution of "stretch" for the variable $K=[\text{momentum}\times\cos\text{ of dip}]^{-1}$ of the scattered proton for events with stopping recoil proton.

Particular care was taken to be sure that the data from hand measurements, and those which were mechanically measured, were compatible. All variables of interest, for each kind of event type, were plotted separately from both sources and compared. No significant differences were found.

The final numbers of events were

2089 elastic events
833 π^+ production
441 π^0 production.

III. RESULTS

A. Cross Sections

About one-half of all rolls were used to obtain cross sections for processes (1)–(3) ($2p$ events). These rolls were all triple scanned for events and double scanned for

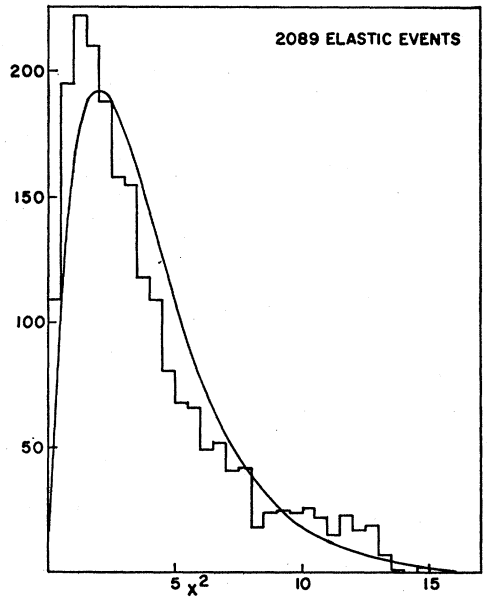

FIG. 7. χ^2 distribution for elastic events (4-constraint events).

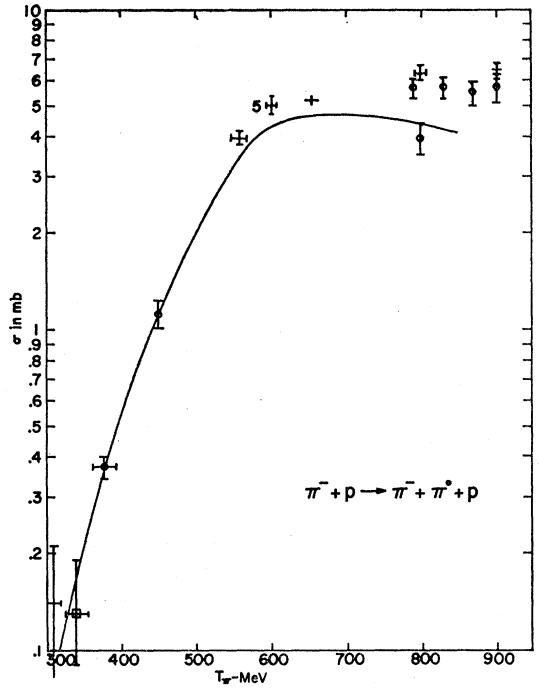

FIG. 8. Excitation function for the reaction $\pi^-+p\rightarrow\pi^-+\pi^0+p$. The result of this experiment is given by point number 5. The smooth curve is the prediction of the Olsson-Yodh model, Ref. 7. The other experimental points are from a compilation which can be found in the University of Maryland Technical Report No. 379 listed in Ref. 7.

track count. For reactions (4) and (5) ($0p$ events) only 3 rolls were scanned using only frames with less than 15 tracks per frame. This was done to check consistency with accurate counter results from Saclay.[4,5] The correction for $\mu-e$ contamination, scanning efficiency, and dip was made separately for determining the $0p$ and the $2p$ cross sections. Table I gives the experimental results. The cross sections σ were evaluated from the equation

$$N=N_tN_0\rho l\eta_1\eta_2\eta_3\sigma,$$

where N_t is the total number of tracks, l is the average track length = 19.3 cm, ρ is the hydrogen density = 0.060 $\pm$0.003 g/cm^3, η_1 is the correction for $\mu-e$ contamination = 0.82$\pm$0.03, η_2 is the correction for dipping tracks = 0.94$\pm$0.01, η_3 is the correction for interactions = 0.987, N is the number of events corrected for scanning efficiency, and N_0 is Avogadro's number. The correction η_2 for dipping tracks is made for the beam tracks as the events were selected in dip as described in the previous section.

TABLE I. Summary of experimental results.

Reaction products	Events	Incident tracks	Cross section (mb)	Counter exp. (mb)
2 charged prongs[a]	1523.4±39.8	95547	30.5±2.1	
π^-+p (elastic)[a,b]	2092		18.9±1.0	18.2±0.5[a]
$\pi^-+\pi^0+p$[a,b]	441		4.0±0.5	
$\pi^-+\pi^++n$[a,b]	833		7.5±0.8	
Neutrals	77.9±9	8473.4	15.5±1.9	12.8±0.5[a]
Multipion production	<2	95547	<40μ[b]	
Total cross section			46.0±2.9	43.3±1.0[a]

[a] These cross sections are derived from σ_{2p} by using the branching proportions (elastic) : (π^0 production) : (π^+ production) = 1 : 0.211 : 0.398.
[b] Scanning efficiency correction has been included.

In Figs. 8 and 9 is a summary of all existing data on the reactions (2) and (3). Our measurements are in good agreement with previous values of the total, elastic, and inelastic cross sections.[3–6]

B. Elastic Angular Distribution

The elastic angular distribution was corrected for efficiency of finding events by comparing different scans of the same film as described in Sec. II, as well as by examining the distribution of the normal to the scattering plane around the beam direction. These azimuth plots are shown for different center of mass scattering angles in Fig. 10. A correction was made where indicated and the angular distribution so obtained is shown in Fig. 11.

A least-squares fit to the angular distribution using the polynomial expansion

$$\frac{d\sigma}{d\omega}=\sum_n A_n\cos^n\theta$$

was made. It was found that powers of cosθ greater

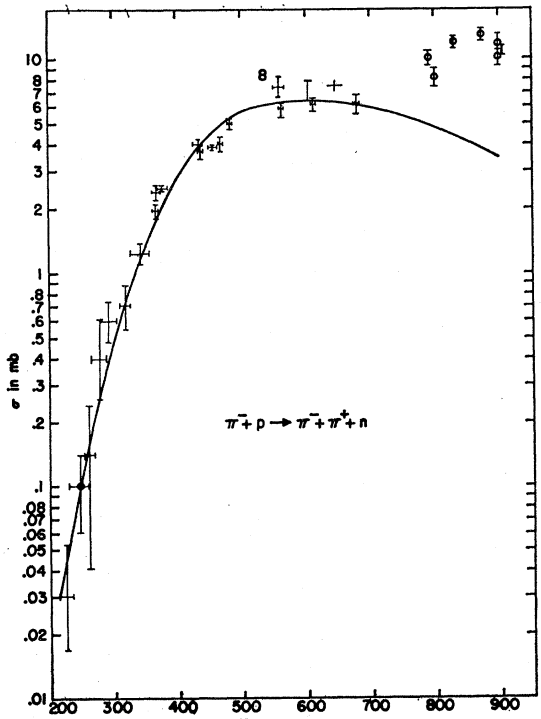

FIG. 9. Excitation function for the reaction $\pi^-+p\rightarrow\pi^-+\pi^++n$, the result of this experiment is given by point number 8. Smooth curve is the prediction of Olsson-Yodh model. The other experimental points are from a compilation which can be found in the University of Maryland Technical Report No. 379 listed in Ref. 7.

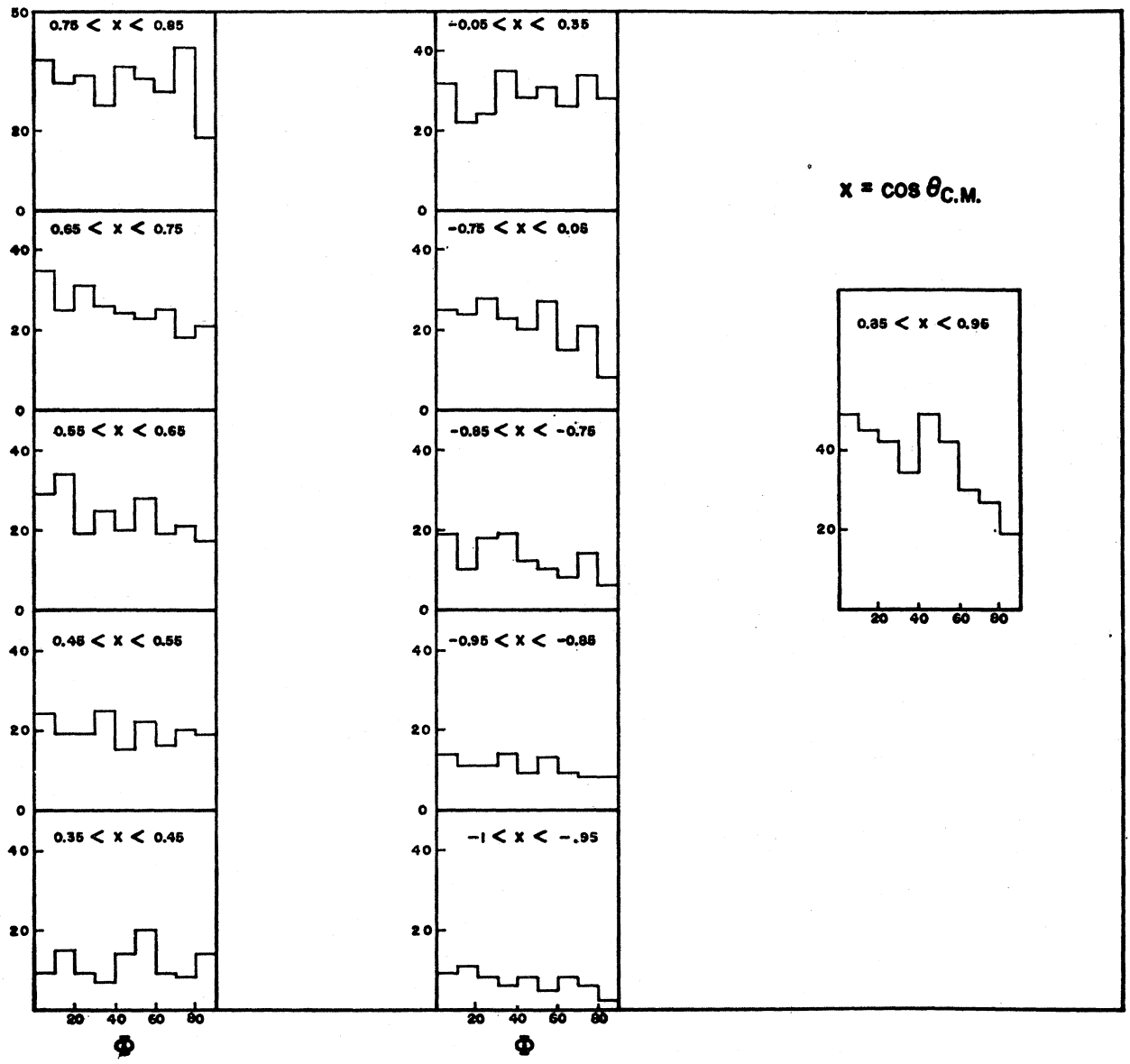

FIG. 10. Azimuthal distributions of the plane of elastic scattering events for different ranges of center-of-mass scattering angle.

than $n=2$ were not required. The fit with $a_0+a_1\cos\theta+a_2\cos^2\theta$ had a $(\chi^2/d)^{1/2}$ of 1.02, where d is the number of degrees of freedom. The differential cross section is given by

$$d\sigma/d\omega=(0.384\pm0.026)+(1.70\pm0.06)\cos\theta+(3.36\pm0.11)\cos^2\theta \text{ mb/sr},$$

which is in good agreement with the previous values of Helland *et al.*[12] The extrapolated value at 0° is consistent with the dispersion theory value from total cross section data.[13]

[12] J. Helland, T. Devlin, D. Hagge, M. Longo, B. J. Moyer, and C. D. Wood, Phys. Rev. Letters **10**, 27 (1963).
[13] See for example J. W. Cronin, Phys. Rev. **118**, 824 (1960).

C. Reaction $\pi^- + p \rightarrow \pi^- + \pi^0 + p$

The distribution of events on Dalitz plot for single π^0 production reactions is shown in Fig. 12. The striking feature of this plot is the depletion of events for the region of low (π^-,π^0) Q values and an enhancement for large (π^-,π^0) Q values. The projections on the three axes: (π^-,p), (π^0,p), and (π^-,π^0) Q values, are shown in Fig. 13. The center-of-mass angular distributions for π^-, π^0, and p are shown in Fig. 14.

The data in these figures are compared with theoretical analysis of Olsson and Yodh[7] (the curves have been normalized to the total number of $\pi^-\pi^0 p$ events). The Olsson-Yodh model assumes that these reactions are dominated by attractive rescattering between pairs

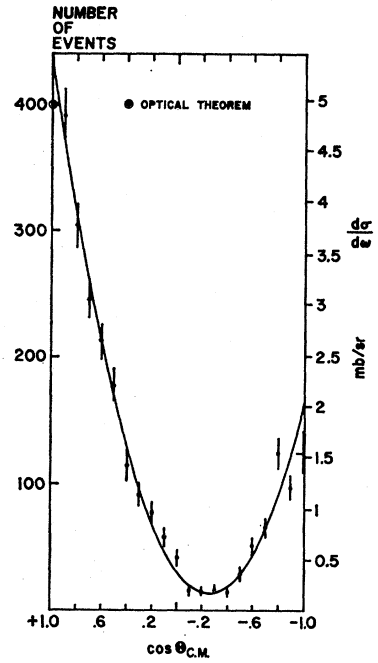

FIG. 11. Elastic angular distribution. The smooth curve is the best fit to the angular distribution.

of final-state particles. The only important attractive scattering states between π and N at these energies are the $T=\frac{1}{2}$, $J^p=\frac{1}{2}^-(\alpha_1)$ and $T=\frac{3}{2}$, $J^p=\frac{3}{2}^+(\delta_{33})$ states. The model also assumes that the extra pion is in the lowest angular-momentum state: $l=0$. Thus, the incoming angular-momentum states included in the model are $p_{1/2}{}^+$ and $d_{3/2}{}^-$ leading to s-wave production of α_1 rescattering and s-wave production of $\delta_{3,3}(N^*(1238))$, respectively. The model takes into account the Bose symmetry of the two pions and the p-wave decay of the $N^*(1238)$. These states must be considered for both $T=\frac{1}{2}$ and $T=\frac{3}{2}$ isotopic-spin states of the π^-+p system. The Olsson-Yodh model predicts a cross section of 3.5 ± 0.5 mb for reaction (2), in good agreement with the experimental value. The event distribution on the Dalitz plot is accounted for satisfactorily by the Olsson-Yodh model. In the π^-, π^0 reaction the $p_{1/2}{}^+$ contribution to the cross section state is very small in the model; thus, there could be other partial waves contributing a corresponding small amount to the cross section. The effects of such admixture will be negligible on the Dalitz plot. However, the angular distributions would be significantly affected by such admixtures. Thus, it is not surprising that the angular distributions in Fig. 14 do not agree with the model prediction. It should be noted that there is no necessity for introducing any $\pi-\pi$ interaction for this state. In this charge-state $\pi-\pi$ isotopic spin can be 1 or 2 but not 0. Thus, any $T=0\pi\pi$ interaction (discussed below) will not affect this system. The ρ exchange model,[14] does not fit the experimental data.

D. Reaction $\pi^-+p\rightarrow\pi^-+\pi^+ +n$

The Olsson-Yodh model predicts a cross section which is within 1 mb (out of 7.5) of the experimental cross section.

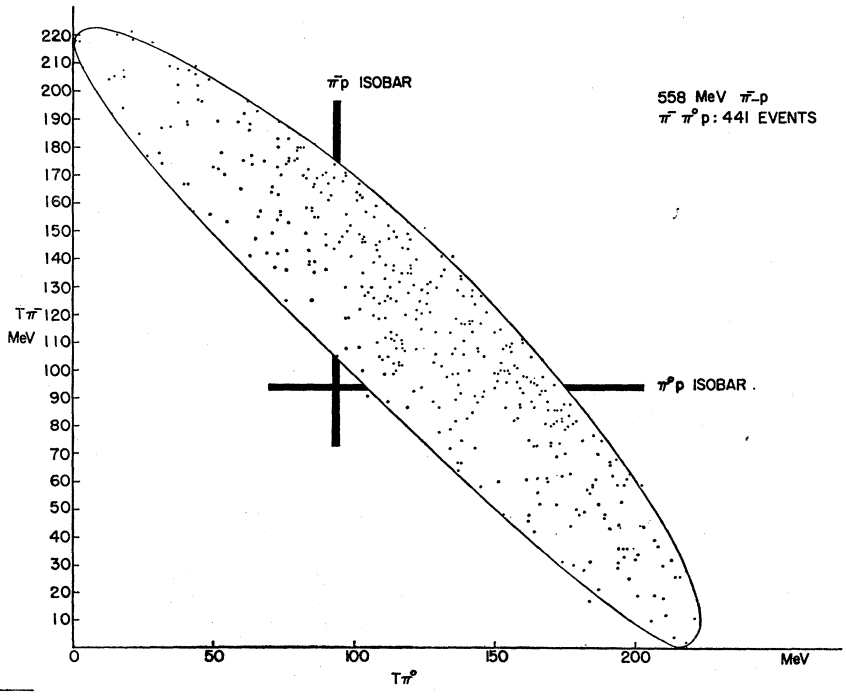

FIG. 12. Dalitz plot for $\pi^-+p\rightarrow\pi^-+\pi^0+p$.

[14] L. Stodolsky and J. J. Sakurai, Phys. Rev. Letters **11**, 90 (1963).

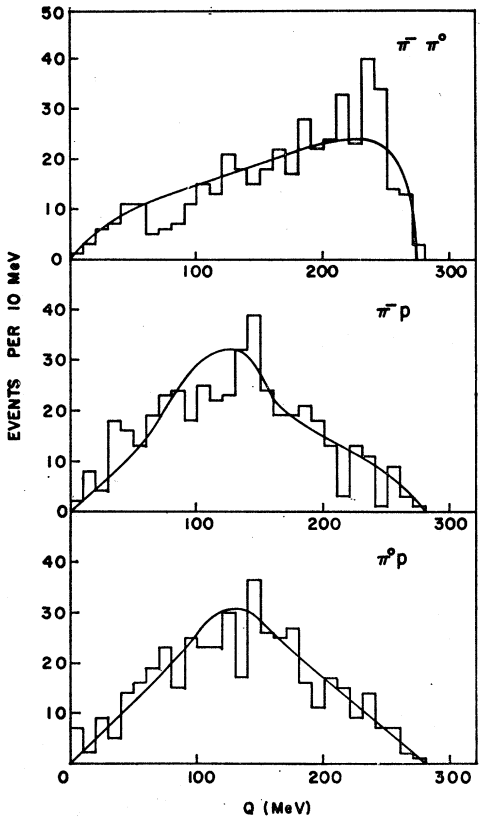

FIG. 13. Projections of events on Dalitz plot on $\pi^-\pi^0$, π^-p, and π^0p axes. The smooth curves are calculated from the Olsson-Yodh model.

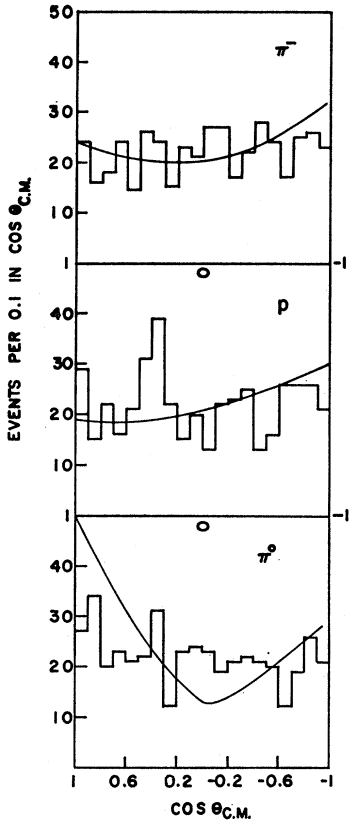

FIG. 14. Center-of-mass angular distribution for π^-, p, and π^0 reaction (2). The model predictions are seen to give an inadequate explanation of the data (see text).

The Dalitz plot for this reaction is shown in Fig. 15. As the $\pi^- - n$ system can resonate in a pure $T=\frac{3}{2}$ state, the $(N^*)^-$ should be more prominent than the $(N^*)^+$.

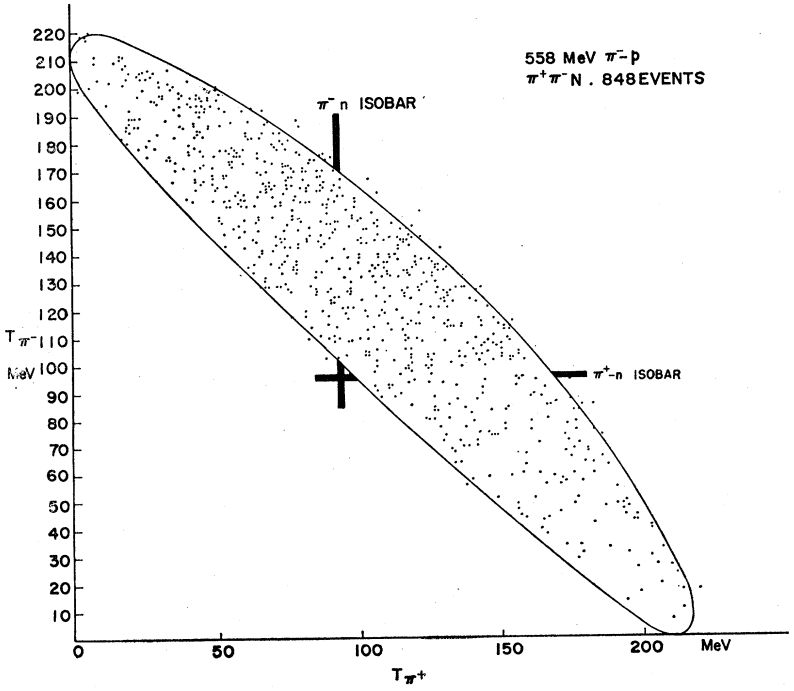

FIG. 15. The Dalitz plot for reaction $\pi^- + p \rightarrow \pi^- + \pi^+ + n$.

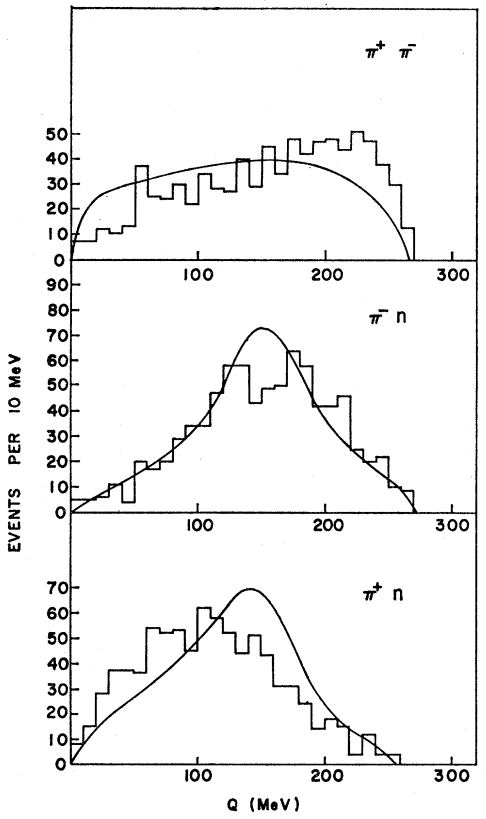

FIG. 16. Projections of events on Dalitz plot on the $\pi^-\pi^+$, π^-n, and π^+n axes. The model accounts for the π^-n distribution but fails to do so for the π^+n or $\pi^+\pi^-$ distributions (see text).

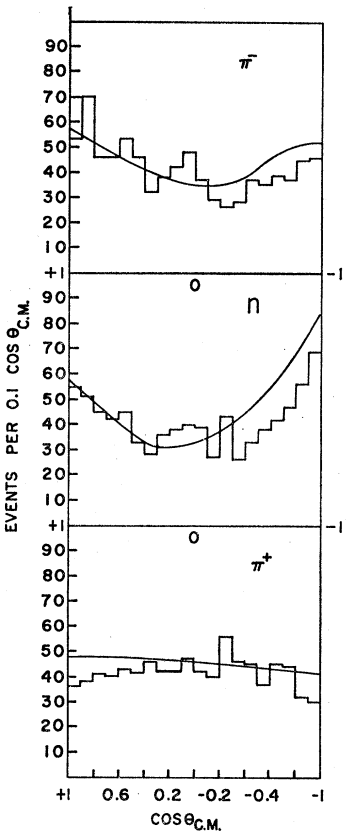

FIG. 17. Center of mass angular distribution for π^-, n, and π^+ of reaction (3). The model predictions show the general features of the angular distributions but the agreement is fair (see text).

This clearly shows up in the Dalitz plot density distribution. There is also a concentration of points in the region of large (π^+,π^-) effective masses. In Fig. 16 the projections on the (π^-,n), (π^+,n), and (π^+,π^-) axes are shown. The curves in Fig. 16 are theoretical predictions of the Olsson-Yodh model under the same assumptions as made for the $\pi^-\pi^0p$ system. It is seen that the model, as developed so far, does not adequately account for the observed Q-value distributions. The projection on the π^-n axis, which shows the dominance of $(N^*)^-$, is adequately explained by the model. However, the model predicts no peaking at maximum $(\pi^-,\pi^+)Q$ values, and the theoretical curve for the π^+n projection peaks at too high a value for $(\pi^+,n)Q$.[15]

In Fig. 17 the center-of-mass angular distributions for the π^-, π^+, and n are shown. The theoretical curves give a fair description of the observed distributions, although the fit is by no means good. The predicted total cross section is also in agreement with data, as stated above. Therefore, it seems that the admixture of other states or $\pi\pi$ rescattering effects must be small. Work is in progress in which the Olsson-Yodh model is extended to include other incoming partial waves and/or a $T=0$ $\pi\pi$ rescattering (or resonance). The peaking for high $\pi^+\pi^-$ masses may be due to the contribution of triangle graphs as pointed out by Anisovich.[16]

[15] Our results for the reaction $\pi^-\pi^+n$ are in good agreement with those of J. Kirz, J. Schwartz and R. D. Tripp, Phys. Rev. **130**, 2481 (1963), who had about half the number of events at this energy. Their cross section is included in Fig. 9.

ACKNOWLEDGMENTS

We wish to acknowledge the excellent cooperation of the 14-in. bubble chamber crew and the Brookhaven National Laboratory Cosmotron staff who made the experiment possible.

The experiment was planned in collaboration with Dr. J. Ashkin. We want to thank Dr. J. Ashkin, Dr. E. G. Pewitt, Dr. T. Fields, and J. Oliver, who participated in setting up the beam, in obtaining the pictures, and in the early phases of the analysis which was done at Carnegie Institute of Technology. The help of Dr. Charles Vittitoe and Dr. V. P. Kenney in beam tracing is gratefully acknowledged. The DATPRO program was supplied to us by Dr. B. Musgrave and Dr. L. Leipuiner. The interest of Dr. R. K. Adair in setting up this parasitic facility to investigate the $\pi-p$ inelastic channels below 1 BeV was most appreciated. One of us (T. B. Day) would like to thank Dr. Z. Slawsky of the Naval Ordnance Laboratory for arranging computing facilities on their 7090.

[16] V. V. Anisovich and L. G. Dakhno, Phys. Letters **10**, 221 (1964).